ACS Catalysis

RESEARCH ARTICLE

pubs.acs.org/acscatalysis

Luminescence-Decay as an Easy-to-Use Tool for the Study of Lanthanide-Containing Catalysts in Aqueous Solutions

Prabani Dissanayake, Yujiang Mei, and Matthew J. Allen*

Department of Chemistry, Wayne State University, Detroit, Michigan 48202, United States

Supporting Information

ABSTRACT: Luminescence-decay measurements were studied as a simple and fast technique to determine inner-sphere water coordination numbers of Ln^{III}-based complexes in binary solvent systems that are useful for catalysis. The luminescence-decay rates of Eu^{III}-containing complexes were used to elucidate the coordination environment of Eu^{III} in these solvent systems. Our findings were used to empirically derive easy-to-use equations to determine the average number of inner-sphere water and solvent molecules in binary aqueous solvent systems. The increased knowledge of the inner-sphere coordination environment of catalysts that our equations enable can be used to study lanthanide-catalyzed reactions and new precatalysts.

KEYWORDS: luminescence-decay, inner-sphere, water-coordination number, lanthanide, catalysis, europium

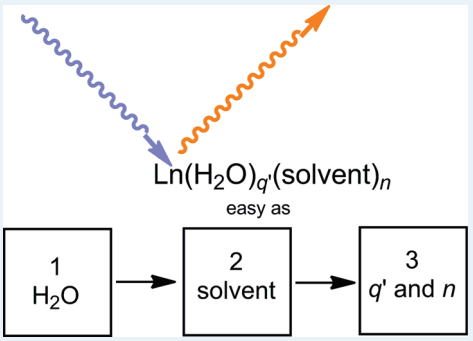

INTRODUCTION

There is a great interest in performing catalytic, stereoselective carbon−carbon and carbon−heteroatom bond-forming reactions in aqueous media.[1−22] Advantages of using moisture-stable catalysts include the ability to use unprotected functional groups, the ease of product separation and catalyst recovery, and the avoidance of costly solvent drying procedures.[23,24] However, most enantioselective Lewis acid precatalysts must be used under strictly anhydrous conditions to avoid hydrolysis. Lanthanide trifluoromethanesulfonates (triflates), $Ln(OTf)_3$, are water-tolerant Lewis acid precatalysts that can catalyze a wide range of important carbon−carbon and carbon−heteroatom bond-forming reactions.[21−23,26−33] Despite the desirable features of these lanthanide-based precatalysts, the use of lanthanide triflates in asymmetric carbon−carbon bond formation in aqueous conditions has been limited by a lack of techniques for gaining a mechanistic understanding of these precatalysts in aqueous catalysis. In this article, we describe a simple method to study lanthanide-catalyzed reactions in commonly used solvent systems.

Recently, we reported the determination of the water-coordination number of lanthanide triflates at intermediate stages of the Mukaiyama aldol reaction in water/tetrahydrofuran (THF) mixtures using luminescence-decay measurements.[34] Furthermore, we reported the use of this technique to study equilibrium with respect to substrate binding and to convey structural information about a new class of precatalysts for asymmetric bond formation.[21] Our initial studies demonstrated the usefulness of this technique with respect to gaining a detailed mechanistic picture of catalysts in solution.

Our initial studies used the luminescent Eu^{III} ion and Horrocks's equation (eq 1), which relates water coordination number to the measured difference in luminescence quenching between O−H and O−D oscillators.[34,35] In this equation, q is the number of water molecules bound directly to the metal (inner-sphere) in 100% water; A is an empirically derived proportionality constant; ${\tau_{H_2O}}^{-1}$ and ${\tau_{D_2O}}^{-1}$ are the measured luminescence-decay rates in H_2O and D_2O; and α represents quenching due to vibrational oscillators present outside the first coordination sphere of Eu^{III}. Here, we will refer to both outer- and second-sphere molecules as outer-sphere.

$$q = A(|{\tau_{H_2O}}^{-1} - {\tau_{D_2O}}^{-1}| - \alpha) \quad (1)$$

Equation 1 was empirically derived in water, and consequently, is not applicable to all solvent systems that are useful for catalysis because of differences in the inner- and outer-sphere luminescence quenching ability between water and other solvents. As a result of these differences, every experiment must be validated when water is not the only solvent. For example, in determining the effect of THF on q values, we performed validation experiments using complexes with known coordination numbers.[34] The additional workload resulting from the need to validate each solvent composition renders the use of Horrocks's equation impractical for the routine study of carbon−carbon and carbon−heteroatom bond-forming reactions in the most commonly used aqueous solvent systems.

Studies have been performed that address the use of luminescence decay in solvents other than water;[36−38] however, these studies have been limited with respect to usefulness for the

Received: April 25, 2011
Revised: July 7, 2011
Published: August 24, 2011

Scheme 1. Synthetic Route to Complex 4

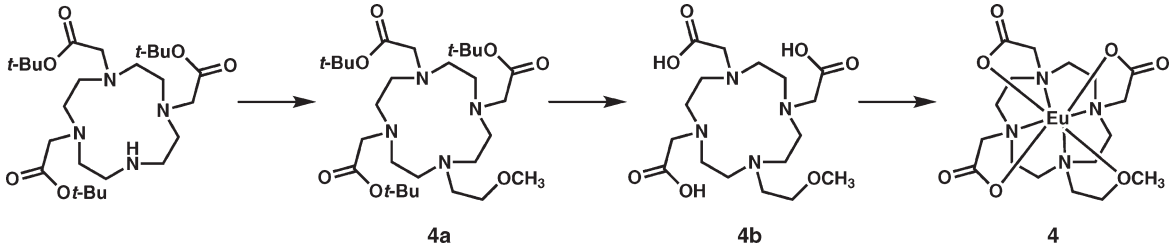

routine study of catalysis. In one example, specific hydroxo complexes were identified in a 1:4 H_2O/dimethylsulfoxide (DMSO) solution.[37] The limited solvent scope and use of a laser make these protocols unattractive for routine use in catalysis research. In another study, Eu^{III} ions were used to determine a correlation between luminescence lifetime and water percentage.[38] The limitation of this report to the study of catalysis lies in the narrow solvent scope (only dimethylformamide (DMF) and DMSO were used with $\leq$1% H_2O) and the Eu^{III} species studied (only perchlorates were studied). Finally, Kimura and co-workers explored solvent coordination to Eu^{III} using solvent mixtures to relate luminescence lifetime to water-coordination number.[36,39,40] However, in their studies, the contribution of inner- and outer-sphere nonwater solvent molecules was neglected; consequently, their results are inaccurate for studying catalysis. Our goal in this paper is to expand upon our previous work[34] to enable practical, routine analysis of lanthanide catalysts with respect to commonly used water-miscible solvents.

Here, we present our studies of the variations of inner- and outer-sphere dynamics with respect to commonly used organic solvents for Lewis acid-mediated catalytic systems including THF, EtOH, MeOH, DMF, DMSO, acetone, and acetonitrile. Furthermore, we discuss empirically derived equations that resulted from our studies and enable fast and accurate determination of inner-sphere coordination behavior in commonly used binary solvent systems. Finally, we validate and demonstrate the use of the equations by comparison to the accepted Horrocks equation[35] and our previous study of the aqueous, lanthanide-catalyzed Mukaiyama aldol reaction.[34] The equations presented in this article are critical to the incorporation of luminescence-decay measurements as routine characterization of lanthanide-catalyzed reactions.

EXPERIMENTAL SECTION

Materials. Commercial chemicals of reagent-grade purity or better were used without purification unless otherwise noted. Water was purified using a PURELAB Ultra Mk2 water purification system (ELGA). THF was purified using a solvent purification system (Vacuum Atmospheres Company). Ethanol was distilled from calcium hydride.[41] Tris(2,6-pyridinedicarboxylate)-europium(III) (**1**),[42] 1,4,7,10-tetraazacyclododecane-1,4,7,10-tetrayltetramethylenetetra(benzylphosphinate)europium(III) (**2**),[43] 2,2′,2″,2‴-(1,4,7,10-tetraazacyclododecane-1,4,7,10-tetrayl)tetra-acetoeuropium(III) (**3**),[44] 2,2′,2″-(1,4,7,10-tetraazacyclododecane-1,4,7-triyl)triacetoeuropium(III) (**5**),[45] and 2,2′-(1,7-dioxa-4,10-diazacyclododecane-4,10-diyl)dipropanoeuropium(III) (**6**)[21] were synthesized following published procedures.

Characterization. ^{1}H NMR spectra were obtained using a Varian Mercury 400 (400 MHz) spectrometer, and ^{13}C NMR spectra were obtained using a Varian Mercury 400 (101 MHz) spectrometer. Chemical shifts are reported relative to residual solvent signals unless otherwise noted ($CDCl_3$: ^{1}H: δ 7.27, ^{13}C: δ 77.23; D_2O: ^{1}H: δ 4.79, ^{13}C: δ 39.51 from an internal standard of dimethyl sulfoxide-d_6). ^{1}H NMR data are assumed to be first order with apparent singlets and multiplets reported as "s" and "m", respectively. Italicized elements are those that are responsible for the shifts. High-resolution electrospray ionization mass spectra (HRESIMS) were obtained on an electrospray time-of-flight high-resolution Waters Micromass LCT Premier XE mass spectrometer. IR spectra were measured using KBr pellets from 4000 to 400 cm^{-1} on a Bruker TENSOR 27 FTIR spectrophotometer. IR maximum absorption peaks are reported in cm^{-1} where the absorptions are s, strong; vs, very strong; and br, broad. Liquid chromatography and mass spectrometry (LC−MS) analysis was performed on a Shimadzu LC−MS system equipped with a C18 column (Restek International, Viva C18, 5 μm, 250 × 4.6 mm), using a binary gradient method (pump A: water; pump B: acetonitrile; 5−95% B over 70 min; flow rate: 1.0 mL/min). Exponential, linear, logarithmic, polynomial, and power trend line options as well as best fit equations were obtained using Microsoft Excel version 2007.

2,2′,2″-(10-(2-Methoxyethyl)-1,4,7,10-tetraazacyclododecane-1,4,7-triyl)triacetoeuropium(III) (4) (Scheme 1). To a mixture of *tert*-butyl 2,2′,2″-(1,4,7,10-tetraazacyclododecane-1,4,7-triyl)triacetate (179 mg, 0.348 mmol, 1 equiv) and anhydrous K_2CO_3 (247 mg, 1.79 mmol, 5 equiv) in anhydrous acetonitrile (10 mL) under an atmosphere of Ar was added 2-bromoethylmethylether (164 μL, 1.75 mmol, 5 equiv). The resulting mixture was stirred at 70 °C for 12 h. After cooling to ambient temperature and removing solids by filtration, the solvent was removed under reduced pressure. The crude product was purified using silica gel chromatography (10:1 dichloromethane/methanol) to yield 194 mg (97%) of the methoxyethyl-functionalized product **4a** as a light yellow oil. ^{1}H NMR (400 MHz, $CDCl_3$, δ): 1.20−1.50 (m, CH_3, 27H), 1.60−3.60 (m, CH_3 and CH_2, 29H); ^{13}C NMR (101 MHz, $CDCl_3$, δ): 27.9 (CH_3), 28.0 (CH_3), 53.0 (CH_2), 56.9 (CH_2), 57.2 (CH_2), 58.9 (CH_3), 68.6 ($C(CH_3)_3$), 81.9 (CH_2), 82.0 (CH_2), 171.9; TLC: R_f = 0.36 (18:1 dichloromethane/methanol); IR (KBr, cm^{-1}): 2978−2830 (s, CH, aliphatic), 1729, 1673 (vs, ester); HRESIMS (m/z): $[M + H]^+$ calcd for $C_{29}H_{57}N_4O_7$, 573.4227; found, 573.4215.

A solution of the methoxyethyl-functionalized product **4a** (99 mg, 0.17 mmol) in an aqueous solution of HCl (12 M, 7.5 mL) was stirred at ambient temperature for 2 h. The reaction mixture was concentrated under reduced pressure, and the resulting residue was dissolved in H_2O (3 mL) and freeze-dried to afford 70 mg (99%) of ligand **4b** as a white solid. ^{1}H NMR (400 MHz, D_2O, δ): 2.90−3.22 (m, CH_2, 8H), 3.26−3.28

dx.doi.org/10.1021/cs200213a |ACS Catal. 2011, 1, 1203–1212

Table 1. Wavelengths Used in the Determination of Inner-Sphere Water-Coordination Numbers

complex	λ_{ex} (nm)	λ_{em} (nm)
1	397	593
2	395	595
3	395	594
4	395	594
5	395	592
6	394	591
$Eu(OTf)_3$	394	591

(m, CH_3, 3H), 3.32−3.66 (m, CH_2, 14H), 3.68−3.76 (m, CH_2, 2H), 4.17 (s, CH_2, 2H); ^{13}C NMR (101 MHz, D_2O, δ): 49.4 (CH_2), 49.9 (CH_2), 52.4 (CH_2), 53.4 (CH_2), 54.4 (CH_2), 55.0 (CH_2), 56.1 (CH_2), 60.2 (CH_3), 67.3 (CH_2), 170.0, 175.6; IR (KBr, cm^{-1}): 3410 (vs, br, OH), 1725 (vs, carboxylic acid), 1661 (s, carboxylic acid); HRESIMS (m/z): $[M - H]^-$ calcd for $C_{17}H_{31}N_4O_7$, 403.2193; found, 403.2205.

To a solution of ligand **4b** (20 mg, 48 mmol, 1 equiv) in H_2O (3 mL) was added $EuCl_3 \cdot 6H_2O$ (39.0 mg, 106 mmol, 2.2 equiv), and the resulting reaction mixture was stirred at ambient temperature for 24 h while maintaining the pH of the reaction mixture between 6.9 and 7.1 with 0.1 M aqueous NH_4OH. The pH of the mixture was increased to 12 using aqueous NH_4OH (14.8 M) to precipitate excess Eu^{III} as $Eu(OH)_3$. The $Eu(OH)_3$ was removed by filtration through a 0.2 μm filter (Millipore, IC Millex-LG), and the filtrate was freeze-dried. The resulting white solid was dissolved in 3 mL of H_2O and dialyzed against H_2O (cellulose ester, 100−500 Da molecular weight cut off, Spectra/Por Biotech), and the dialysate was changed after 3, 7, and 17 h. After dialysis, the solution inside the membrane was freeze-dried to yield 26 mg (83%) of **4** as a white solid. The purity of the product was confirmed by LC−MS (Supporting Information); IR (KBr, cm^{-1}): 1628, 1405; HRESIMS (m/z): $[M + H]^+$ calcd for $C_{17}H_{30}N_4O_7{}^{151}Eu$, 553.1317; found 553.1313.

Luminescence-Decay Measurements. Luminescence-decay measurements were performed using a HORIBA Jobin Yvon Fluoromax-4 spectrofluorometer. Solutions (1 mM) of $Eu(OTf)_3$ and solutions of Eu^{III} complexes **1**−**6** were prepared using binary aqueous mixtures as solvents. Cosolvents included THF, EtOH, MeOH, DMSO, acetone, or acetonitrile. Water was used at 1, 2, 3, 4, 5, 6, 7, 8, 9, 10, 20, 30, 40, 50, 60, 70, 80, 90, and 100% (v/v) with each cosolvent for a total of 109 unique solvent systems. Sample preparation was repeated with D_2O mixtures of THF, ethanol-d, methanol-d_4, DMSO, acetone, and acetonitrile. Prior to dissolving the Eu^{III}-containing samples in deuterated solvent systems, the samples were repeatedly (3×) dissolved in D_2O and concentrated to dryness under reduced pressure. The sample preparation was also repeated with DMF/H_2O and DMF-d_7/D_2O at 1, 3, 5, 9, 20, 60, 90, and 100% (v/v) H_2O or D_2O, respectively.

Samples were sealed in cuvettes that were purged with Ar prior to filling. Luminescence-decay measurements were acquired using the excitation (λ_{ex}) and emission (λ_{em}) wavelengths for the $^7F_0 \rightarrow {}^5D_0$ transitions listed in Table 1. All other parameters were kept constant during the luminescence-decay measurements [excitation and emission slit widths (5 nm), flash count (100), initial delay (0.001 ms), maximum delay (2 ms), and delay increment (0.02 ms)]. The decay rates (τ^{-1}) were obtained as the slopes of plots of the natural log of luminescence intensity versus time. This procedure was performed for every solution, and all solutions were independently prepared and measured three to nine times. The resulting mean decay rates have standard errors ≤0.05 ms^{-1}.

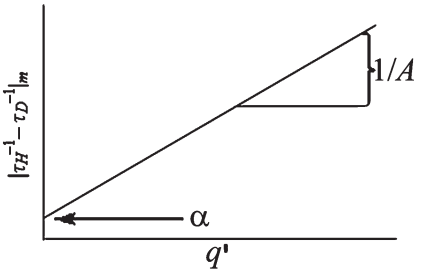

Figure 1. Plot of $|\tau_H^{-1} - \tau_D^{-1}|_m$ versus q' used to determine α and A. The intercept of the plot is α, and the reciprocal of the slope is the proportionality constant A.

RESULTS AND DISCUSSION

When water-miscible organic solvents are used with water in binary solvents in lanthanide-catalyzed organic transformations, the inner- and outer-sphere coordination environments of the lanthanide ions become complex relative to the coordination environment in water. Specifically, when water-miscible solvents occupy the inner-coordination sphere, the luminescence quenching arising from inner-sphere vibrations and the number of inner-sphere water molecules are different from the same complexes in only water. While it is likely that complexes **1**−**6** exist as multiple species (hydroxides, hydrates, and oxides) in equilibrium in solution, these complexes displayed a single peak for the $^7F_0 \rightarrow {}^5D_0$ transition; therefore, we assumed that the Eu^{III} complexes in this study existed in a single form or that different forms were in equilibrium to give an average value of q'. The mono-exponential luminescence decay values that we obtained for both H_2O and D_2O solutions ($R^2 \geq 0.99$) further support our assumption.[35,46] We will refer to the number of inner-sphere water molecules in binary solvent systems as q'. Determination of q' is important because the number of inner-sphere water molecules plays an important role in the mechanism of the aqueous lanthanide-based catalysis.[21,34] However, application of the empirically derived Horrocks equation (eq 1)[35] to determine q' is limited because eq 1 was derived in the absence of cosolvents. To determine q', we have examined changes to the parameters in Horrocks's equation (α and A) with respect to commonly used binary solvent systems. Using a similar strategy as Horrocks, we plotted $|\tau_H^{-1} - \tau_D^{-1}|_m$, which is the difference of the measured decay rates in protic and deuterated solvent systems, against q' (Figure 1). This plot enabled us to determine new α and A values in binary solvents using eq 2, which describes the data in Figure 1. However, we could not directly adapt Horrocks's method because of the complications to luminescence decay arising from both inner-and outer-sphere nonwater solvent molecules.

$$|\tau_H^{-1} - \tau_D^{-1}|_m = \frac{1}{A}q' + \alpha \qquad (2)$$

To overcome the difficulties associated with nonwater solvent molecules, we developed a six-step procedure to solve for q' and the nonwater inner-sphere solvent-coordination number, which we will refer to as n, in binary solvent systems. This stepwise procedure was applied to complexes **1**−**6** (Figure 2) as well as

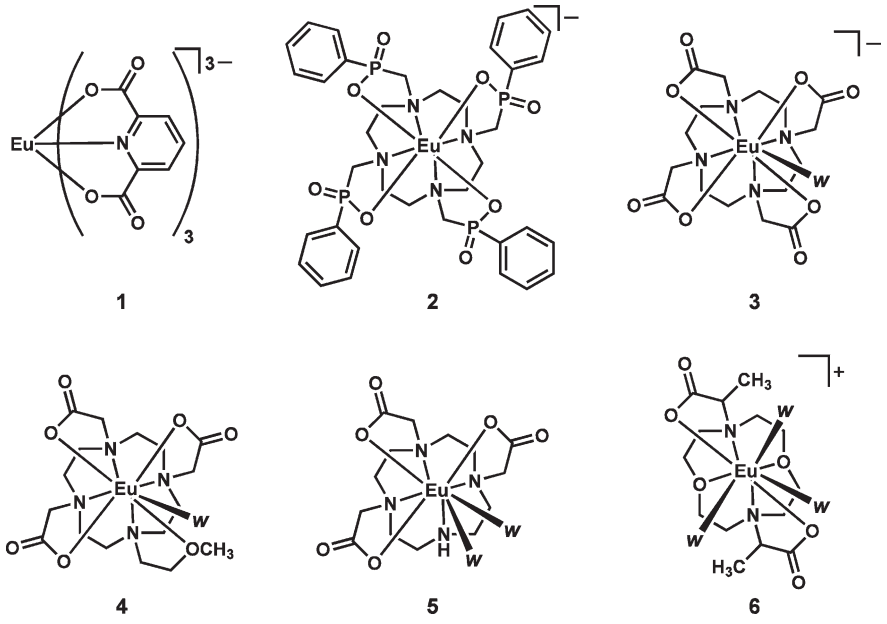

Figure 2. Studied complexes with *w* values ranging from 0 to 3, where *w* represents coordination sites that remain after ligand binding.

$Eu(OTf)_3$. These complexes were chosen because they represent a range (0−3 and 9) of well-defined numbers of coordination sites that remain after ligand coordination, which we will define as *w*. The use of complexes that span a wide range of *w* values is important because it enables our results to be used for any lanthanide-based precatalysts. Values of *w* were obtained from published values,[43,47−51] but because complexes **4** and **6** did not have published coordination numbers, the number of open sites was established as 1 and 3, respectively, using *q* measurements in H_2O.[35] Additionally, because not all of the complexes were soluble in every solvent system studied, we used multiple complexes for some values of *w*: complex **1** or **2** for *w* values of zero and complex **3** or **4** for *w* values of one. The six-step procedure is described followed by a description of our validation of the resulting equations, an example of the use of our results to study a known system, and a flowchart that we expect will enable our results to be used routinely by the scientific community.

Step 1. Measure the luminescence-decay rates of Eu^{III} complexes of known values of *w* in commonly used binary solvent systems with water percentages ranging from 1 to 100%. The observed decay rates are a combination of both inner- and outer-sphere decay as illustrated by eq 3, where $|\tau_H^{-1} - \tau_D^{-1}|_{IS}$ is the absolute value of the difference of luminescence-quenching rates due to inner-sphere solvent molecules and $|\tau_H^{-1} - \tau_D^{-1}|_{OS}$ is the absolute value of the difference of luminescencel.-quenching rates due to outer-sphere molecules. The measured values of $|\tau_H^{-1} - \tau_D^{-1}|_m$ have maximum values in 100% water, and these values generally decrease with decreasing water concentration (Tables 2−8). This decrease is likely due to the presence of both inner- and outer-sphere non-water solvent molecules that have a smaller per-molecule contribution to luminescence decay compared to water.

$$|\tau_H^{-1} - \tau_D^{-1}|_m = |\tau_H^{-1} - \tau_D^{-1}|_{IS} + |\tau_H^{-1} - \tau_D^{-1}|_{OS} \quad (3)$$

Step 2. Measure the luminescence-decay rate caused by outer-sphere molecules using Eu^{III} complexes **1** and **2** that are composed of ligands that saturate the inner-coordination sphere of the metal. By completely blocking the inner-coordination sphere ($|\tau_H^{-1} - \tau_D^{-1}|_{IS} = 0$ in eq 3), we were able to isolate and measure luminescence decay caused by outer-sphere solvent molecules as illustrated in eq 4.

$$|\tau_H^{-1} - \tau_D^{-1}|_m = |\tau_H^{-1} - \tau_D^{-1}|_{OS} \quad (4)$$

The results obtained for Step 2 are included in Tables 2−8 ($w = 0$). The luminescence decay caused by outer-sphere solvent molecules were maximum in 100% water, and these values

Table 2. Mean $|\tau_H^{-1} - \tau_D^{-1}|_m$ Values for MeOH and Methanol-d_4

	$\lvert\tau_H^{-1} - \tau_D^{-1}\rvert_m$ (ms^{-1})				
% (v/v) of H_2O in MeOH or D_2O in methanol-d_4	**1** or **2** ($w = 0$)	**3** ($w = 1$)	**5** ($w = 2$)	**6** ($w = 3$)	$Eu(OTf)_3$ ($w = 9$)
100	0.35[a]	1.15	1.99	2.79	7.84
90	0.35[a]	1.11	1.87	2.66	7.56
80	0.35[a]	1.08	1.80	2.64	7.43
70	0.33[a]	1.07	1.64	2.63	7.21
60	0.30[a]	1.06	1.52	2.50	7.13
50	0.30[a]	0.98	1.45	2.49	7.12
40	0.30[a]	0.96	1.35	2.38	7.09
30	0.29[a]	0.96	1.30	2.37	6.96
20	0.25[a]	0.96	1.31	2.34	6.81
10	0.22[a]	0.93	1.32	2.31	6.48
9	0.21[a]	0.93	1.28	2.31	6.36
8	0.16[a]	0.92	1.22	2.25	6.31
7	0.14[a]	0.91	1.20	2.29	6.21
6	0.12[a]	0.89	1.20	2.24	6.21
5	0.12[b]	0.85	1.17	2.24	5.93
4	0.12[b]	0.84	1.16	2.13	5.44
3	0.10[b]	0.82	1.17	1.92	5.35
2	0.10[b]	0.81	1.08	1.86	5.00
1	0.10[b]	0.80	1.01	1.84	4.87

[a] Complex **1**. [b] Complex **2**.

dx.doi.org/10.1021/cs200213a |*ACS Catal.* 2011, 1, 1203–1212

Table 3. Mean $|\tau_H^{-1} - \tau_D^{-1}|_m$ Values for EtOH and Ethanol-*d*

% (v/v) of H_2O in EtOH or D_2O in ethanol-*d*	$\|\tau_H^{-1} - \tau_D^{-1}\|_m$ (ms^{-1})				
	1 or **2**	**3**	**5**	**6**	$Eu(OTf)_3$
	($w = 0$)	($w = 1$)	($w = 2$)	($w = 3$)	($w = 9$)
100	0.35[a]	1.15	1.99	2.79	7.84
90	0.28[a]	1.07	1.82	2.70	7.56
80	0.27[a]	1.05	1.68	2.66	7.46
70	0.25[a]	1.03	1.66	2.64	7.35
60	0.21[a]	1.01	1.61	2.60	7.29
50	0.22[a]	0.98	1.59	2.60	7.26
40	0.20[a]	0.97	1.54	2.56	7.10
30	0.20[a]	0.97	1.55	2.50	7.04
20	0.27[a]	0.93	1.50	2.43	6.79
10	0.25[a]	0.87	1.45	2.46	6.56
9	0.24[a]	0.87	1.35	2.46	6.41
8	0.13[a]	0.87	1.33	2.50	6.40
7	0.12[a]	0.83	1.34	2.48	6.39
6	0.11[b]	0.86	1.32	2.45	6.40
5	0.11[b]	0.76	1.32	2.35	6.09
4	0.10[b]	0.75	1.15	2.22	5.56
3	0.10[b]	0.77	1.18	1.90	5.23
2	0.10[b]	0.76	1.16	1.88	5.15
1	0.10[b]	0.75	1.15	1.87	5.15

[a] Complex **1**. [b] Complex **2**.

Table 4. Mean $|\tau_H^{-1} - \tau_D^{-1}|_m$ Values for DMSO

% (v/v) of H_2O or D_2O in DMSO	$\|\tau_H^{-1} - \tau_D^{-1}\|_m$ (ms^{-1})				
	1	**3**	**5**	**6**	$Eu(OTf)_3$
	($w = 0$)	($w = 1$)	($w = 2$)	($w = 3$)	($w = 9$)
100	0.35	1.15	1.99	2.79	7.84
90	0.30	1.08	1.47	1.91	6.66
80	0.24	0.88	1.33	1.46	6.25
70	0.22	0.87	1.21	1.52	5.40
60	0.20	0.81	0.98	1.56	4.46
50	0.19	0.76	0.84	1.36	3.82
40	0.18	0.67	0.74	1.27	3.42
30	0.17	0.58	0.66	0.94	2.64
20	0.14	0.33	0.44	0.72	1.21
10	0.12	0.22	0.26	0.35	0.68
9	0.12	0.17	0.23	0.35	0.68
8	0.10	0.14	0.20	0.32	0.68
7	0.08	0.13	0.17	0.30	0.64
6	0.06	0.13	0.17	0.31	0.64
5	0.04	0.12	0.16	0.23	0.49
4	0.01	0.03	0.04	0.10	0.29
3	0.01	0.02	0.04	0.08	0.21
2	0.01	0.01	0.03	0.05	0.16
1	0.01	0.01	0.03	0.05	0.14

decreased with decreasing concentration of water. These results provide further evidence that nonwater outer-sphere solvent molecules contribute less to luminescence quenching than water on a per-molecule basis.

Step 3. Calculate the inner-sphere decay component by subtracting the outer-sphere component (the data obtained from Step 2) from the measured data in Step 1. The isolated inner-sphere component is composed of decay arising from water molecules and nonwater solvent molecules (eq 5), where $|\tau_H^{-1} - \tau_D^{-1}|_{IS_{water}}$ is the inner-sphere decay rate difference per proto and deuterowater molecule and $|\tau_H^{-1} - \tau_D^{-1}|_{IS_{solvent}}$ is the inner-sphere decay rate difference per nonwater solvent molecule. The isolated $|\tau_H^{-1} - \tau_D^{-1}|_{IS}$ is the sum of $|\tau_H^{-1} - \tau_D^{-1}|_{IS_{water}}$ multiplied by the number of coordinated water molecules (q') and $|\tau_H^{-1} - \tau_D^{-1}|_{IS_{solvent}}$ multiplied by the number of coordinated solvent molecules (n). Representative results obtained for Step 3 are shown for DMSO in Table 9 (see Supporting Information for other solvents). Complexes **1** and **2** have been omitted because the value of $|\tau_H^{-1} - \tau_D^{-1}|_{IS}$ for these complexes is 0 by definition.

$$|\tau_H^{-1} - \tau_D^{-1}|_{IS} = q'|\tau_H^{-1} - \tau_D^{-1}|_{IS_{water}} + n|\tau_H^{-1} - \tau_D^{-1}|_{IS_{solvent}} \quad (5)$$

Step 4. Determine the inner-sphere decay rate difference per molecule in the absence of water. To determine the values of the per-molecule decay rate differences in eq 5, one of the two differences was set to zero for the $Eu(OTf)_3$ samples. In this step, we set $q' = 0$ in eq 5 by using each cosolvent in the absence of water (eq 6).

$$|\tau_H^{-1} - \tau_D^{-1}|_{IS} = n|\tau_H^{-1} - \tau_D^{-1}|_{IS_{solvent}} \quad (6)$$

In eq 6, n can be replaced by w when $q' = 0$, using the relationship shown in eq 7, where w equals the total number of coordinated water and solvent molecules. When n was replaced by w, eq 8 was obtained, and $|\tau_H^{-1} - \tau_D^{-1}|_{IS_{solvent}}$ for each solvent was divided by 9 (the w value of $Eu(OTf)_3$), as described in eq 9, to calculate the inner-sphere decay rate per solvent molecule for all of the solvents studied. The calculated $|\tau_H^{-1} - \tau_D^{-1}|_{IS_{solvent}}$ values

Table 5. Mean $|\tau_H^{-1} - \tau_D^{-1}|_m$ Values for Acetone

% (v/v) of H_2O or D_2O in acetone	$\|\tau_H^{-1} - \tau_D^{-1}\|_m$ (ms^{-1})				
	1 or **2**	**3** or **4**	**5**	**6**	$Eu(OTf)_3$
	($w = 0$)	($w = 1$)	($w = 2$)	($w = 3$)	($w = 9$)
100	0.35[a]	1.15[d]	1.99	2.79	7.84
90	0.30[a]	1.05[d]	1.84	2.77	7.60
80	0.29[a]	1.04[d]	1.80	2.70	7.53
70	0.30[a]	1.04[d]	1.77	2.66	7.51
60	0.29[a]	1.04[d]	1.75	2.61	7.36
50	0.28[a]	1.02[d]	1.72	2.60	7.17
40	0.26[a]	1.02[d]	1.70	2.54	6.94
30	0.25[a]	0.98[d]	1.69	2.49	6.77
20	0.21[b]	0.96[d]	1.64	2.47	6.79
10	0.20[b]	0.96[d]	1.59	2.44	6.79
9	0.19[b]	0.95[d]	1.46	2.39	6.80
8	0.18[b]	0.94[d]	1.37	2.34	6.80
7	0.18[b]	0.87[d]	1.30	2.25	6.69
6	0.16[b]	0.84[d]	1.29	2.22	6.62
5	0.16[b]	0.86[d]	1.26	2.20	6.63
4	ns[c]	0.84[e]	ns[c]	2.01	6.35
3	ns[c]	0.73[e]	ns[c]	1.98	5.98
2	ns[c]	0.71[e]	ns[c]	1.94	5.85
1	ns[c]	0.69[e]	ns[c]	1.89	5.76

[a] Complex **1**. [b] Complex **2**. [c] ns = not soluble. [d] Complex **3**. [e] Complex **4**.

dx.doi.org/10.1021/cs200213a |*ACS Catal.* 2011, 1, 1203–1212

Table 6. Mean $|\tau_H^{-1} - \tau_D^{-1}|_m$ Values for THF

% (v/v) of H_2O or D_2O in THF	$\lvert\tau_H^{-1} - \tau_D^{-1}\rvert_m$ (ms^{-1})				
	1 or **2** ($w = 0$)	**3** or **4** ($w = 1$)	**5** ($w = 2$)	**6** ($w = 3$)	$Eu(OTf)_3$ ($w = 9$)
100	0.35[a]	1.15[d]	1.99	2.79	7.84
90	0.30[a]	1.10[d]	1.88	2.66	7.55
80	0.30[a]	1.08[d]	1.88	2.63	7.45
70	0.29[a]	1.07[d]	1.75	2.65	7.47
60	0.29[a]	1.08[d]	1.78	2.63	7.44
50	0.28[a]	1.15[d]	1.63	2.62	7.36
40	0.27[a]	1.15[d]	1.63	2.67	7.33
30	0.25[a]	1.15[d]	1.61	2.68	7.36
20	0.23[a]	1.15[d]	1.61	2.65	7.38
10	0.19[b]	0.98[d]	1.51	2.61	7.11
9	0.19[b]	0.94[d]	1.46	2.54	6.93
8	0.16[b]	0.92[d]	1.49	2.58	6.93
7	0.16[b]	0.92[d]	1.44	2.57	6.96
6	0.14[b]	0.92[d]	1.49	2.61	6.97
5	0.13[b]	0.92[d]	1.45	2.58	6.80
4	ns[c]	0.99[e]	1.41	2.58	6.86
3	ns[c]	0.99[e]	1.50	ns[c]	6.79
2	ns[c]	0.91[e]	1.03	ns[c]	5.26
1	ns[c]	0.91[e]	1.00	ns[c]	5.19

[a] Complex **1**. [b] Complex **2**. [c] ns = not soluble. [d] Complex **3**. [e] Complex **4**.

Table 7. Mean $|\tau_H^{-1} - \tau_D^{-1}|_m$ Values for Acetonitrile

% (v/v) of H_2O or D_2O in acetonitrile	$\lvert\tau_H^{-1} - \tau_D^{-1}\rvert_m$ (ms^{-1})				
	1 or **2** ($w = 0$)	**3** or **4** ($w = 1$)	**5** ($w = 2$)	**6** ($w = 3$)	$Eu(OTf)_3$ ($w = 9$)
100	0.35[a]	1.15[d]	1.99	2.79	7.84
90	0.31[a]	1.06[d]	1.80	2.76	7.59
80	0.29[a]	1.06[d]	1.53	2.76	7.50
70	0.29[a]	1.05[d]	1.57	2.73	7.50
60	0.29[a]	1.01[d]	1.49	2.73	7.47
50	0.25[a]	1.01[d]	1.39	2.72	7.44
40	0.26[a]	1.01[d]	1.33	2.68	7.40
30	0.25[a]	1.01[d]	1.33	2.65	7.40
20	0.24[a]	1.01[d]	1.30	2.64	7.37
10	0.26[b]	1.07[d]	1.11	2.65	7.21
9	0.26[b]	1.05[d]	1.13	2.54	7.08
8	0.26[b]	1.06[d]	1.13	2.42	6.94
7	0.26[b]	1.09[d]	1.12	2.39	6.82
6	0.26[b]	1.04[d]	1.14	2.35	6.62
5	0.20[b]	0.93[d]	ns[c]	2.06	6.60
4	0.20[b]	0.93[e]	ns[c]	2.08	6.59
3	ns[c]	0.89[e]	ns[c]	1.83	6.17
2	ns[c]	0.79[e]	ns[c]	1.79	5.89
1	ns[c]	0.70[e]	ns[c]	1.56	5.34

[a] Complex **1**. [b] Complex **2**. [c] ns = not soluble. [d] Complex **3**. [e] Complex **4**.

are listed in Table 10.

$$q' + n = w \tag{7}$$

$$|\tau_H^{-1} - \tau_D^{-1}|_{IS} = w|\tau_H^{-1} - \tau_D^{-1}|_{IS_{solvent}} \tag{8}$$

$$\frac{|\tau_H^{-1} - \tau_D^{-1}|_{IS}}{w} = |\tau_H^{-1} - \tau_D^{-1}|_{IS_{solvent}} \tag{9}$$

We observed values of zero for the decay per inner-sphere solvent molecule for THF, DMSO, DMF, acetonitrile, and acetone. This result is likely because these solvents do not contain vibrational oscillators capable of quenching the Eu^{III} excited state energy. For MeOH and EtOH, decay per inner-sphere solvent molecule values were greater than zero because of the presence of O−H oscillators.

Step 5. Repeat Step 4 using 100% water to determine the inner-sphere decay rate per water molecule when no cosolvent is present ($n = 0$ from eq 5). Here q' in eq 5 was replaced by w to obtain eq 10, and eq 11 shows the rearrangement of eq 10 used to calculate the inner-sphere decay rate per water molecule. The calculated $|\tau_H^{-1} - \tau_D^{-1}|_{IS_{water}}$ value is listed in Table 10.

$$|\tau_H^{-1} - \tau_D^{-1}|_{IS} = w|\tau_H^{-1} - \tau_D^{-1}|_{IS_{water}} \tag{10}$$

$$\frac{|\tau_H^{-1} - \tau_D^{-1}|_{IS}}{w} = |\tau_H^{-1} - \tau_D^{-1}|_{IS_{water}} \tag{11}$$

The decay per inner-sphere water molecule was approximately twice that of inner-sphere solvent molecules for MeOH and EtOH (Table 10). This observation is not surprising because there are half as many O−H oscillators in MeOH or EtOH as there are in water.

Table 8. Mean $|\tau_H^{-1} - \tau_D^{-1}|_m$ Values for DMF and DMF-d_7[a]

% (v/v) of H_2O in DMF or D_2O in DMF-d_7	$\lvert\tau_H^{-1} - \tau_D^{-1}\rvert_m$ (ms^{-1})				
	1 ($w = 0$)	**3** ($w = 1$)	**5** ($w = 2$)	**6** ($w = 3$)	$Eu(OTf)_3$ ($w = 9$)
100	0.35	1.15	1.99	2.79	7.84
90	0.35	1.07	1.67	2.13	6.58
60	0.31	0.93	1.29	1.63	5.16
20	0.29	0.61	0.88	1.25	4.18
9	0.24	0.49	0.73	1.09	4.02
5	0.24	0.44	0.69	1.10	3.89
3	0.14	0.23	0.52	0.67	2.43
1	0.10	0.21	0.47	0.64	2.17

[a] Fewer measurements were performed because of the cost of DMF-d_7.

Step 6. Determine q' and n by combining eqs 5 and 12 for each complex in all the studied solvent systems. This determination is important because solving for q' in binary solvent systems is the key step to determination of α and A (Figure 1). It is critical to note here that the measured luminescence-decay rates were due to the experimental number of coordination sites not occupied by a multidentate ligand, w'. This experimental w' is different than w because many of the w values were determined in a static environment using X-ray crystallography, while w' is measured in a dynamic environment. The experimental w' value for each studied complex was calculated by dividing the $|\tau_H^{-1} - \tau_D^{-1}|_{IS}$ values in 100% water by $|\tau_H^{-1} - \tau_D^{-1}|_{IS_{water}}$. All measured w' values are less than or equal to the respective w values (Table 11). Using w' we have rewritten eq 7 as eq 12 to account for solution dynamics. Equation 12 was used with eq 5 and the data from

dx.doi.org/10.1021/cs200213a |ACS Catal. 2011, 1, 1203–1212

Table 9. Mean $|\tau_H^{-1} - \tau_D^{-1}|_{IS}$ Values for DMSO

% (v/v) of H_2O or D_2O in DMSO	$\|\tau_H^{-1} - \tau_D^{-1}\|_{IS}$ (ms^{-1})			
	3 ($w = 1$)	**5** ($w = 2$)	**6** ($w = 3$)	$Eu(OTf)_3$ ($w = 9$)
100	0.80	1.64	2.44	7.49
90	0.78	1.17	1.61	6.36
80	0.64	1.09	1.22	6.01
70	0.65	0.99	1.30	5.18
60	0.61	0.78	1.36	4.26
50	0.57	0.65	1.17	3.63
40	0.49	0.56	1.09	3.24
30	0.41	0.49	0.77	2.47
20	0.19	0.30	0.58	1.07
10	0.10	0.14	0.23	0.56
9	0.05	0.11	0.23	0.56
8	0.04	0.10	0.22	0.58
7	0.05	0.09	0.22	0.56
6	0.07	0.11	0.25	0.58
5	0.08	0.12	0.19	0.45
4	0.02	0.03	0.09	0.28
3	0.01	0.03	0.07	0.20
2	0.00	0.02	0.04	0.15
1	0.00	0.02	0.04	0.13

Table 10. Calculated Decay Rate Per Inner-Sphere Solvent Molecule

solvent	$\|\tau_H^{-1} - \tau_D^{-1}\|_{IS_{water}}$
water	0.83[a]
methanol	0.41
ethanol	0.44
DMSO	0
acetone	0
THF	0
acetonitrile	0
DMF	0

[a] $|\tau_H^{-1} - \tau_D^{-1}|_{IS_{water}}$

Tables 9−11 (and Tables S1−S6 in the Supporting Information for solvents other than DMSO) to create a system of two equations and two variables (q' and n). This system allowed for q' and n to be determined in all of the solvent systems studied. The calculated values of q' and n in the DMSO/water binary system are shown in Table 12 as a representative system. The q' and n values for each complex in all of the studied solvent systems are shown in the Supporting Information.

$$q' + n = w' \tag{12}$$

The maximum calculated q' value was obtained in 100% water for each complex, and these values decreased with decreasing concentration of water. Further, the maximum calculated n values were observed at the lowest water percentages. After calculating q' values, we were able to plot our data to derive α and A using the same strategy as Horrocks and co-workers. To achieve this goal, the $|\tau_H^{-1} - \tau_D^{-1}|_m$ values from Step 1 were

Table 11. Values of w and w' for Complexes 1−6 and $Eu(OTf)_3$

complex	w	w'
1	0	0
2	0	0
3	1	0.96
4	1	0.96
5	2	1.97
6	3	2.95
$Eu(OTf)_3$	9	9.00

plotted against the q' values for complexes **1**−**6** as well as $Eu(OTf)_3$ in all the binary mixtures studied. For complexes in MeOH and EtOH, $|\tau_H^{-1} - \tau_D^{-1}|_m$ values were plotted against $(q' + n/2)$ because these solvents have a decay per solvent molecule that is approximately half that of one water molecule. A representative plot is shown in Figure 3 using the DMSO binary solvent system with 60% water (v/v). The remaining $|\tau_H^{-1} - \tau_D^{-1}|_m$ versus q' and $|\tau_H^{-1} - \tau_D^{-1}|_m$ versus $(q' + n/2)$ plots are shown in the Supporting Information.

The data in Figure 3 and the Supporting Information indicate that decay rates have a linear dependence on q' values in all of the measured solvent systems. Because complexes **1**−**6** and $Eu(OTf)_3$ do not contain nonsolvent ligand-based O−H oscillators, the intercept of these plots can be used to determine changes outside of the inner-sphere (α in eq 1) for each unique binary solvent system (Table 13). Additionally, the A value was calculated as 1.2 using the reciprocal of the slope of the best fit line of the plots. This value was independent of the solvent system.

The results in Table 13 indicate that the maximum value for the outer-sphere contribution to luminescence decay, α, was obtained in 100% water. This is likely because water molecules have more vibrational quenchers (two O−H oscillators) than the other solvents in this study. Furthermore, values of α tend to decrease with decreasing water percentage in each solvent system, and this reduction is proportional to the preferential solvation of the Eu^{III} center.[36,52] Interestingly, values of α for solvents without O−H oscillators were not equivalent. This difference is likely due to the different strengths of the interactions of these solvents with water leading to changes in the vibrations of the water molecules.[53−56] Because these vibrations are responsible for quenching in the outersphere, changes to these vibrations from hydrogen bonding, density, or van der Waals interactions are expected to influence α.

To enable the determination of α at any water percentage, as opposed to the 19 discrete values in this study, the α values from Table 13 were plotted against water percentage (v/v) for each solvent system (plots are shown in the Supporting Information). The best fit equations for each solvent are shown in Table 14.

To check the validity of our empirically derived equations for α relative to the values obtained using Horrocks's equation (eq 1) in 100% water, we recalculated α with $x = 100$ using the equations in Table 14. Our empirically derived α values for 100% water are within the range of 0.31−0.36 (Table 15). We subsequently recalculated the number of inner-sphere water molecules in 100% H_2O for all of the complexes that we studied using the α value that we obtained for 100% H_2O (Results for q' determinations were rounded to two significant figures).[46] This comparison enables us to determine the accuracy of q' values

dx.doi.org/10.1021/cs200213a |ACS Catal. 2011, 1, 1203–1212

Table 12. Calculated q' and n Values for DMSO Binary Systems

	3 (w = 1)		**5** (w = 2)		**6** (w = 3)		$Eu(OTf)_3$ (w = 9)	
% (v/v) of H_2O in DMSO or D_2O in DMSO	q'	n	q'	n	q'	n	q'	n
100	0.96	0.00	1.97	0.00	2.95	0.00	9.00	0.00
90	0.94	0.02	1.41	0.56	1.94	1.01	7.66	1.34
80	0.77	0.19	1.32	0.65	1.48	1.47	7.24	1.76
70	0.79	0.17	1.20	0.77	1.57	1.38	6.25	2.75
60	0.74	0.22	0.94	1.03	1.64	1.31	5.13	3.87
50	0.69	0.27	0.79	1.18	1.41	1.54	4.37	4.63
40	0.59	0.37	0.68	1.29	1.31	1.64	3.91	5.09
30	0.49	0.47	0.59	1.38	0.94	2.01	2.98	6.02
20	0.24	0.72	0.36	1.61	0.70	2.25	1.30	7.70
10	0.13	0.83	0.18	1.79	0.28	2.67	0.68	8.32
9	0.06	0.90	0.14	1.83	0.28	2.67	0.68	8.32
8	0.06	0.90	0.12	1.85	0.27	2.68	0.70	8.30
7	0.06	0.90	0.11	1.86	0.26	2.69	0.68	8.32
6	0.09	0.87	0.13	1.84	0.30	2.65	0.69	8.31
5	0.10	0.86	0.15	1.82	0.23	2.72	0.54	8.46
4	0.02	0.94	0.03	1.94	0.11	2.84	0.34	8.66
3	0.01	0.95	0.04	1.93	0.08	2.87	0.24	8.76
2	0.00	0.96	0.03	1.94	0.05	2.90	0.18	8.82
1	0.00	0.96	0.02	1.95	0.04	2.91	0.15	8.85

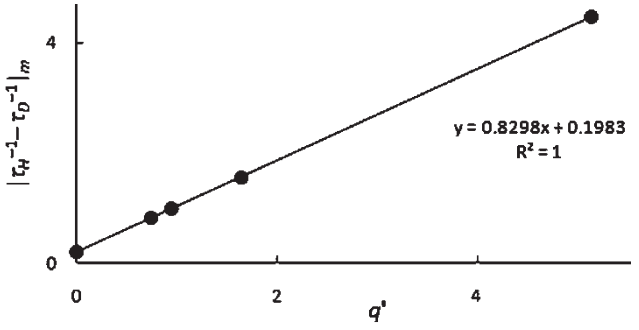

Figure 3. $|\tau_H^{-1} - \tau_D^{-1}|_m$ versus q' for 60% H_2O (v/v) in DMSO.

derived from our equations compared to w values that were obtained from published values.[43,47−51] Further, we extended our recalculations of inner-sphere water molecules in nonwater solvent systems, by using x = 100 (100% H_2O) in our new empirically derived equations for α. Table 15 shows the resulting values that display at most ±0.1 water molecules of uncertainty relative to w. For comparison, we analyzed our data from the 100% water system (water in Table 15) using the commonly accepted Horrocks equation[35] and found w values of 0.12, 1.1, 1.8, 2.7, and 8.3 for **1**, **3**, **5**, **6**, and $Eu(OTf)_3$, respectively. This comparison demonstrates that the calculated values using our equations more closely (±0.1 vs ±0.7) reflect the actual system (w) than the Horrocks equation. It should be noted that our equations can be applied for $w \leq 9$ where Horrocks's equations were only applicable to complexes $w \leq 1$ (α = 0.25) and for $1 < w \leq 6$ (α = 0.31).[35] Our range is extended because we have extended the determination of q' up to nine free coordination sites for Eu^{III} complexes where other studies have stopped at 6.[35]

Table 13. Values of α for Each Binary Solvent System Studied[a]

H_2O% (v/v)	methanol	ethanol	DMSO	acetone	THF	acetonitrile	DMF
100	0.35	0.35	0.35	0.35	0.35	0.35	0.35
90	0.35	0.33	0.30	0.30	0.30	0.31	0.35
80	0.36	0.32	0.29	0.29	0.30	0.30	nd*
70	0.34	0.32	0.24	0.30	0.30	0.29	nd*
60	0.31	0.29	0.20	0.29	0.29	0.29	0.31
50	0.31	0.29	0.19	0.24	0.28	0.25	nd*
40	0.31	0.27	0.18	0.26	0.27	0.24	nd*
30	0.30	0.26	0.17	0.25	0.25	0.23	nd*
20	0.26	0.25	0.12	0.21	0.23	0.21	0.29
10	0.23	0.23	0.12	0.20	0.19	0.19	nd*
9	0.22	0.22	0.12	0.19	0.19	0.18	0.24
8	0.15	0.14	0.09	0.18	0.16	0.18	nd*
7	0.11	0.13	0.08	0.18	0.16	0.17	nd*
6	0.12	0.13	0.06	0.16	0.14	0.17	nd*
5	0.13	0.12	0.04	0.16	0.11	0.13	0.24
4	0.11	0.11	0.01	nd	nd	0.11	nd*
3	0.10	0.11	0.01	nd	nd	nd	0.14
2	0.09	0.11	0.01	nd	nd	nd	nd*
1	0.07	0.11	0.01	nd	nd	nd	0.10

[a] nd = not determined because of insolubility; nd* = not determined because of the cost of DMF-d_7.

It is also worth noting that ligand systems that contain aromatic groups in close proximity to the Eu^{III} ion might display back energy transfer and lead to less accurate determinations of q';[57] however, we did not observe this problem for complex **2**.

dx.doi.org/10.1021/cs200213a |ACS Catal. 2011, 1, 1203–1212

Table 14. Equations Describing α as a Function of Water Percentage[a]

cosolvent	α
methanol	$0.722 \ln x + 0.285$
ethanol	$0.0598 \ln x + 0.055$
DMSO (x = 1−9)	$0.0018x^2 - 0.0033x + 0.0092$
DMSO (x = 10−100)	$10^{-5x^2} + 0.001x + 0.1051$
acetone	$0.1132x^{0.2219}$
THF	$0.064 \ln x + 0.0301$
acetonitrile	$0.0587 \ln x + 0.0427$
DMF	$0.0523 \ln x + 0.1123$

[a] The variable x is the water percentage (v/v).

Table 15. Recalculated α and Inner-Sphere Water Molecules in 100% H_2O for All the Complexes

solvent	α	1 (w = 0)	3 (w = 1)	5 (w = 2)	6 (w = 3)	$Eu(OTf)_3$ (w = 9)
water	0.35	0.00	0.96	2.0	2.9	9.0
DMF	0.35	0.00	0.96	2.0	2.9	9.0
acetonitrile	0.31	0.05	1.0	2.0	3.0	9.0
THF	0.32	0.03	0.99	2.0	3.0	9.0
acetone	0.31	0.05	1.0	2.0	3.0	9.0
DMSO	0.31	0.05	1.0	2.0	3.0	9.0
ethanol	0.33	0.02	0.98	2.0	3.0	9.0
methanol	0.36	0.00	0.95	2.0	3.0	9.0

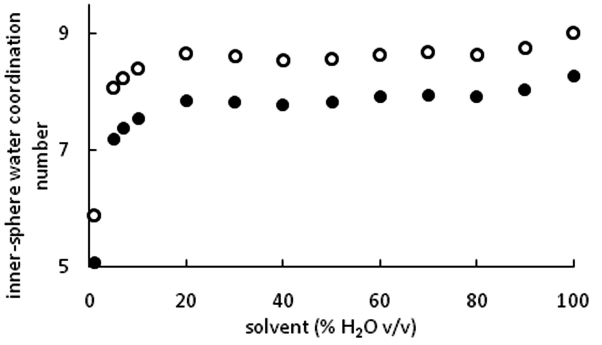

Figure 4. Comparison between published q values taken from ref 7 (●) and recalculated q' (○) of Eu^{III} in the first reaction coordinate of the catalytic cycle. Standard error bars are smaller than the size of the dots.

To demonstrate an application of our empirically derived equations, we have recalculated the water-coordination measurements from an earlier study.[34] Figure 4 shows the previously published q and recalculated q' values of the first reaction coordinate of Eu^{III} in the catalytic cycle of the Mukaiyama aldol reaction.[58] The recalculated q' values were significantly different at a 95% confidence interval (student's t test) from the published q values. Further, an increase of up to 0.9 in water-coordination number was observed upon application of our empirically derived A and α values to determine q'. The increased q' values at low water percentages are due to both reduced α values and an increased A value. The observed increase of q' values at higher water percentages is due to an increased A value. However, the use of our recalculated q' values are more appropriate for THF/water binary systems because of the consideration of solvent effects.

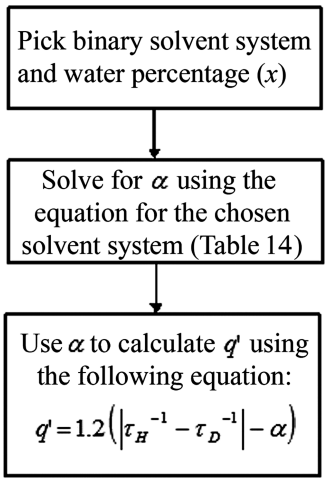

Figure 5. Flowchart description of our new simple method to determine the number of inner-sphere water molecules of a Eu^{III} complex in a binary solvent system.

Finally, we have derived a simple three-step procedure for applying our results to the study of lanthanide-catalyzed reactions. The equations listed in Table 14 can be applied easily to study the water-coordination number of any Ln^{III}-based precatalyst (via the Eu^{III} analogue) that does not contain O−H or N−H oscillators coordinated to the metal ion. These equations are useful for studying precatalysts that are soluble in any water percentage in the binary systems studied using the three-step flowchart in Figure 5.

CONCLUSION

We have empirically derived equations that enable fast and accurate determination of the water-coordination number of lanthanides in synthetically useful binary solvent systems. This determination is extremely important to understand the dynamics of the inner- and outer-sphere environments of Ln^{III}-based precatalysts in aqueous solvent mixtures that can enable the easy acquisition of mechanistic and structural information regarding water-tolerant catalysts. The present work opens a gateway for the study of any lanthanide-catalyzed reaction and is a powerful tool for catalyst design.

ASSOCIATED CONTENT

Supporting Information. Calculated mean $|\tau_H^{-1} - \tau_D^{-1}|_{IS}$ values; calculated q' and n values; $|\tau_H^{-1} - \tau_D^{-1}|_m$ versus q' or $(q' + n/2)$ plots; intercept versus solvent (% H_2O v/v) plots; LC−MS chromatogram of complex **4**; and calculated q' for intermediates in the Mukaiyama aldol reaction. This material is available free of charge via the Internet at http://pubs.acs.org.

AUTHOR INFORMATION

Corresponding Author
*E-mail: mallen@chem.wayne.edu.

Funding Sources
This research was supported by startup funds from Wayne State University (WSU) and a CAREER Award from the National

Science Foundation (CHE-0955000). P.D. was supported by a Heller Fellowship from WSU.

REFERENCES

(1) Xu, S.; Wang, Z.; Zhang, X.; Ding, K. *Eur. J. Org. Chem.* **2011**, 110–116.
(2) Egami, H.; Oguma, T.; Katsuki, T. *J. Am. Chem. Soc.* **2010**, *132*, 5886–5895.
(3) Hu, S.; Li, J.; Xiang, J.; Pan, J.; Luo, S.; Cheng, J.-P. *J. Am. Chem. Soc.* **2010**, *132*, 7216–7228.
(4) Wang, B.; Liu, X.-w.; Liu, L.-y.; Chang, W.-x.; Li, J. *Eur. J. Org. Chem.* **2010**, 5951–5954.
(5) Ghosh, S. K.; Zheng, Z.; Ni, B. *Adv. Synth. Catal.* **2010**, *352*, 2378–2382.
(6) Mao, Z.; Jia, Y.; Li, W.; Wang, R. *J. Org. Chem.* **2010**, *75*, 7428–7430.
(7) Brown, C. J.; Bergman, R. G.; Raymond, K. N. *J. Am. Chem. Soc.* **2009**, *131*, 17530–17531.
(8) He, R.; Shirakawa, S.; Maruoka, K. *J. Am. Chem. Soc.* **2009**, *131*, 16620–16621.
(9) De Nisco, M.; Pedatella, S.; Ullah, H.; Zaidi, J. H.; Naviglio, D.; Özdamar, Ö.; Caputo, R. *J. Org. Chem.* **2009**, *74*, 9562–9565.
(10) Nagano, T.; Kobayashi, S. *J. Am. Chem. Soc.* **2009**, *131*, 4200–4201.
(11) Lu, J.; Liu, F.; Loh, T.-P. *Adv. Synth. Catal.* **2008**, *350*, 1781–1784.
(12) Mase, N.; Watanabe, K.; Yoda, H.; Takabe, K.; Tanaka, F.; Barbas, C. F., III *J. Am. Chem. Soc.* **2006**, *128*, 4966–4967.
(13) Hayashi, Y.; Sumiya, T.; Takahashi, J.; Gotoh, H.; Urushima, T.; Shoji, M. *Angew. Chem., Int. Ed.* **2006**, *45*, 958–961.
(14) Ooi, T.; Uematsu, Y.; Maruoka, K. *J. Am. Chem. Soc.* **2006**, *128*, 2548–2549.
(15) Gu, Y.; Ogawa, C.; Kobayashi, J.; Mori, Y.; Kobayashi, S. *Angew. Chem., Int. Ed.* **2006**, *45*, 7217–7220.
(16) Kobayashi, S.; Ogawa, C. *Chem.—Eur. J.* **2006**, *12*, 5954–5960.
(17) Lemay, M.; Ogilvie, W. W. *Org. Lett.* **2005**, *7*, 4141–4144.
(18) Nishikata, T.; Yamamoto, Y.; Gridnev, I. D.; Miyaura, N. *Organometallics* **2005**, *24*, 5025–5032.
(19) Hamada, T.; Manabe, K.; Kobayashi, S. *J. Am. Chem. Soc.* **2004**, *126*, 7768–7769.
(20) Hamada, T.; Manabe, K.; Kobayashi, S. *Angew. Chem., Int. Ed.* **2003**, *42*, 3927–3930.
(21) Mei, Y.; Dissanayake, P.; Allen, M. J. *J. Am. Chem. Soc.* **2010**, *132*, 12871–12873.
(22) Hamada, T.; Manabe, K.; Ishikawa, S.; Nagayama, S.; Shiro, M.; Kobayashi, S. *J. Am. Chem. Soc.* **2003**, *125*, 2989–2996.
(23) Kobayashi, S.; Hachiya, I. *J. Org. Chem.* **1994**, *59*, 3590–3596.
(24) Eckert, C. A.; Liotta, C. L.; Bush, D.; Brown, J. S.; Hallett, J. P. *J. Phys. Chem. B* **2004**, *108*, 18108–18118.
(25) Gupta, M.; Paul, S.; Gupta, R. *Curr. Sci.* **2010**, *99*, 1341–1360.
(26) Procopio, A.; Costanzo, P.; Curini, M.; Nardi, M.; Oliverio, M.; Paonessa, R. *Synthesis* **2011**, *1*, 73–78.
(27) Arimitsu, S.; Hammond, G. B. *J. Org. Chem.* **2006**, *71*, 8665–8668.
(28) Cameron, L. L.; Wang, S. C.; Kluger, R. *J. Am. Chem. Soc.* **2004**, *126*, 10721–10726.
(29) Touchard, V.; Graillat, C.; Boisson, C.; D'Agosto, F.; Spitz, R. *Macromolecules* **2004**, *37*, 3136–3142.
(30) Isobe, Y.; Fujioka, D.; Habaue, S.; Okamoto, Y. *J. Am. Chem. Soc.* **2001**, *123*, 7180–7181.
(31) Satoh, K.; Kamigaito, M.; Sawamoto, M. *Macromolecules* **2000**, *33*, 4660–4666.
(32) Yu, L.; Li, J.; Ramirez, J.; Chen, D.; Wang, P. G. *J. Org. Chem.* **1997**, *62*, 903–907.
(33) Chen, D.; Yu, L.; Wang, P. G. *Tetrahedron Lett.* **1996**, *37*, 4467–4470.
(34) Dissanayake, P.; Allen, M. J. *J. Am. Chem. Soc.* **2009**, *131*, 6342–6343.
(35) Supkowski, R. M.; Horrocks, W. D., Jr. *Inorg. Chim. Acta* **2002**, *340*, 44–48.
(36) Kimura, T.; Nagaishi, R.; Kato, Y.; Yoshida, Z. *J. Alloys Compd.* **2001**, *323−324*, 164–168.
(37) Sánchez-Lombardo, I.; Andolina, C. M.; Morrow, J. R.; Yatsimirsky, A. K. *Dalton Trans.* **2010**, *39*, 864–873.
(38) Lis, S.; Choppin, G. R. *Anal. Chem.* **1991**, *63*, 2542–2543.
(39) Kimura, T.; Kato, Y. *J. Alloys Compd.* **1998**, *275−277*, 806–810.
(40) Kimura, T.; Kato, Y. *J. Alloys Compd.* **1995**, *225*, 284–287.
(41) Armarego, W. L. F.; Chai, C. L. L. Purification of Organic Chemicals. *Purification of Laboratory Chemicals*, 5th ed.; Elsevier: Cornwall, Great Britain, 2003; pp 231−232.
(42) D'Aléo, A.; Pompidor, G.; Elena, B.; Vicat, J.; Baldeck, P. L.; Toupet, L.; Kahn, R.; Andraud, C.; Maury, O. *Chem. Phys. Chem.* **2007**, *8*, 2125–2132.
(43) Rohovec, J.; Vojtíšek, P.; Hermann, P.; Mosinger, J.; Žák, Z.; Lukeš, I. *Dalton Trans.* **1999**, 3585–3592.
(44) Burai, L.; Tóth, É.; Moreau, G.; Sour, A.; Scopelliti, R.; Merbach, A. E. *Chem.—Eur. J.* **2003**, *9*, 1394–1404.
(45) Kalesse, M.; Loos, A. *Bioorg. Med. Chem. Lett.* **1996**, *17*, 2063–2068.
(46) Andolina, C. M.; Holthoff, W. G.; Page, P. M.; Mathews, R. A.; Morrow, J. R.; Bright, F. V. *Appl. Spectrosc.* **2009**, *63*, 483–493.
(47) Persson, I.; D'Angelo, P.; De Panfilis, S.; Sandström, M.; Eriksson, L. *Chem.—Eur. J.* **2008**, *14*, 3056–3066.
(48) Tóth, É.; Dhubhghaill, O. M. N.; Besson, G.; Helm, L.; Merbach, A. E. *Magn. Reson. Chem.* **1999**, *37*, 701–708.
(49) Brayshaw, P. A.; Bünzli, J.-C. G.; Froidevaux, P.; Harrowfield, J. M.; Kim, Y.; Sobolev, A. N. *Inorg. Chem.* **1995**, *34*, 2068–2076.
(50) Spirlet, M.-R.; Rebizant, J.; Desreux, J. F.; Loncin, M.-F. *Inorg. Chem.* **1984**, *23*, 359–363.
(51) Silber, H. B.; Mioduski, T. *Inorg. Chem.* **1984**, *23*, 1577–1583.
(52) Tanaka, F.; Kawasaki, Y.; Yamashita, S. *J. Chem. Soc., Faraday Trans. 1* **1988**, *84*, 1083–1090.
(53) Holden, C. A.; Hunnicutt, S. S.; Sánchez-Ponce, R.; Craig, J. M.; Rutan, S. C. *Appl. Spectrosc.* **2003**, *57*, 483–490.
(54) Stangret, J. *J. Mol. Struct.* **2002**, *643*, 29–35.
(55) Mosyak, A. A.; Prezhdo, O. V.; Rossky, P. J. *J. Mol. Struct.* **1999**, *485−486*, 545–554.
(56) Dickens, B.; Dickens, S. H. *J. Res. Natl. Inst. Stand. Technol.* **1999**, *104*, 173–183.
(57) Beeby, A.; Faulkner, S.; Parker, D.; Williams, J. A. G. *J. Chem. Soc., Perkin Trans. 2* **2001**, 1268–1273.
(58) See Supporting Information for the published q and recalculated q' of the second and third reaction coordinates of Eu^{III} in the catalytic cycle.